



**HAL**  
open science

## High resolution spectroscopy and a theoretical line list of ethylene between 5000 and 9000 $\text{cm}^{-1}$

S. Mraidi, L. Manceron, H. Aroui, A. Campargue, Michael M. Rey

### ► To cite this version:

S. Mraidi, L. Manceron, H. Aroui, A. Campargue, Michael M. Rey. High resolution spectroscopy and a theoretical line list of ethylene between 5000 and 9000  $\text{cm}^{-1}$ . *Journal of Quantitative Spectroscopy and Radiative Transfer*, 2023, 310, pp.108734. 10.1016/j.jqsrt.2023.108734 . hal-04257888

**HAL Id: hal-04257888**

**<https://hal.science/hal-04257888>**

Submitted on 25 Oct 2023

**HAL** is a multi-disciplinary open access archive for the deposit and dissemination of scientific research documents, whether they are published or not. The documents may come from teaching and research institutions in France or abroad, or from public or private research centers.

L'archive ouverte pluridisciplinaire **HAL**, est destinée au dépôt et à la diffusion de documents scientifiques de niveau recherche, publiés ou non, émanant des établissements d'enseignement et de recherche français ou étrangers, des laboratoires publics ou privés.

# High resolution spectroscopy and a theoretical line list of ethylene between 5000 and 9000 $\text{cm}^{-1}$

S. Mraidi <sup>a</sup>, L. Manceron <sup>b,c</sup>, M. Rey <sup>d</sup>, H. Aroui <sup>a</sup> and A. Campargue <sup>e,\*</sup>

<sup>a</sup> *Laboratoire de Spectroscopie et Dynamique Moléculaire, Ecole Nationale Supérieure d'Ingénieurs de Tunis, Université de Tunis, 5 Av Taha Hussein 1008 Tunis, Tunisia*

<sup>b</sup> *Synchrotron Soleil Ligne AILES, BP 48, 91192 Cedex Gif-sur-Yvette, France*

<sup>c</sup> *LISA, CNRS, Université Paris Cité and Univ Paris Est Creteil, F-75013 Paris, France*

<sup>d</sup> *GSMA, UMR CNRS 7331, University of Reims Champagne Ardenne, Moulin de la Housse B.P. 1039, Cedex Reims, F-51687, France*

<sup>e</sup> *Univ. Grenoble Alpes, CNRS, LIPhy, 38000 Grenoble, France*

**Key words:** ethylene; ethene,  $\text{C}_2\text{H}_4$ ; Fourier transform spectroscopy; TheoReTS

\* Corresponding author: [Alain.Campargue@univ-grenoble-alpes.fr](mailto:Alain.Campargue@univ-grenoble-alpes.fr)

## Abstract

The absorption spectrum of ethylene ( $C_2H_4$ ) in the range 5000-9000  $cm^{-1}$  has been recorded by high-resolution Fourier transform spectroscopy (FTS) at four temperatures (130, 201, 240 and 297 K) and two pressures for each temperature value. The recorded spectra show a very high spectral congestion even at the lowest temperature. Here we present the analysis of a subset of the data limited to a weak absorption interval (6700-7260  $cm^{-1}$ ) at 130 K and 297 K. An empirical list of 12243 lines was retrieved from the 130 K spectrum. Line intensities range between about  $10^{-25}$  and  $10^{-22}$  cm/molecule. In the 7120-7260  $cm^{-1}$  region, a list of 2276 lines was combined to the 130 K list to derive the empirical value of the lower state energy of 1249 transitions from the variation of the line intensity between 130 and 297 K ( $2T$ -method). The line list of  $^{12}C_2H_4$  transitions calculated by the variational method is provided in the 5200-9000  $cm^{-1}$  range (241921 and 179927 transitions at 296 K and 130K, respectively, above intensity cutoff of  $1 \times 10^{-25}$  cm/molecule). This list is an extension of the Theoretical Reims-Tomsk Spectral (TheoReTS) available at lower energy. In spite of the considerable spectral congestion and of significant deviations between the variational and experimental line lists, 647 transitions could be rovibrationally assigned to seven vibrational bands in the FTS spectrum at 130 K between 6700 and 7260  $cm^{-1}$ . The assignments rely on the position and intensity agreement combined with a systematic use of Lower State Combination Difference (LSCD) relations. The comparison between the empirical values of the lower state energy and their exact value provided by the rovibrational assignment is discussed.

## 1. Introduction

Ethylene ( $C_2H_4$ ) or “ethene” according to the IUPAC nomenclature, is a planar molecule with an inversion center. With six atoms, ethylene is the simplest alkene. This colorless molecule is of importance in many fields. Ethylene induces the ripening process for many fruits and is an important pollutant produced by biomass fires [12]. Ethylene is a key species for understanding the physical chemistry of various planetological and astrophysical objects. The  $C_2H_4$  molecule has been detected in Jupiter’s atmosphere [3,4], on Saturn [5,6], on Neptune, and Titan [8-12].

The present contribution aims at providing new quantitative laboratory data on the absorption spectrum of ethylene which are essential for reliable remote sensing. Indeed, there is a lack of high resolution data in the current spectroscopic databases. For instance, the HITRAN database [13] provides line parameters for only two spectral intervals, 620-1530  $cm^{-1}$  and 2929-3242  $cm^{-1}$ , the latter corresponding to the fundamental C-H stretching modes. This situation is partly due to the complexity of the absorption spectrum of ethylene related to its twelve vibrational modes. The analysis of the high resolution ethylene spectra is made extremely challenging above 2000  $cm^{-1}$  because of (i) an unclear polyad scheme, contrary to other small hydrocarbons like methane and (ii) the occurrence of many resonance interactions leading to a structureless highly congested spectrum at room temperature. In fact, although medium resolution (0.5  $cm^{-1}$ ) spectra of  $C_2H_4$  are available in the literature in the region of the CH stretching overtones up to  $V_{CH}= 4$  around 11500  $cm^{-1}$  [14], the most excited region which has been analyzed at high resolution is the first CH stretching overtone region near 6150  $cm^{-1}$ . As visible on the overview spectrum displayed in **Fig. 1**, the absorption in the 1.6  $\mu m$  region is strong and thus suitable for trace detection of ethylene with photoacoustic detection using laser diodes [15,16]. High resolution spectra in the first CH overtone region dominated by the  $\nu_5+\nu_9$  band, were recorded with a variety of experimental approaches including Fourier transform spectroscopy (FTS) both at room temperature and low rotational temperature (53 K) in a slit-jet expansion [17]. In [18], together with an FTS spectrum at room temperature between 6070 and 6230  $cm^{-1}$ , sub-Doppler spectroscopy was performed in a molecular beam with an optothermal detection between 6147 and 6170  $cm^{-1}$ . Parkes et al. [19] and Kapitanov et al. [20] used diode lasers for modulation spectroscopy or cavity ring down spectroscopy (CRDS), respectively, in limited spectral intervals around the center of the  $\nu_5+\nu_9$  band near 6150  $cm^{-1}$ . The most complete analysis in this region was reported by Loroño Gonzalez et al. [21], on the basis of an FTS spectrum and an opto-acoustic spectrum with a diode laser, using an effective model restricted to two interacting vibrational bands. More than 600 lines could be assigned to the  $\nu_5+\nu_9$  and  $\nu_5+\nu_{11}$  stretching dyad and effective Hamiltonian parameters were fitted. Unfortunately, the assignments were limited to the strongest lines and no quantitative intensity information was provided in this reference while line intensities are prerequisites for quantitative trace gas analysis.

To the best of our knowledge, only the CRDS study of Ref. [20] provided absolute line intensities in the region of the  $\nu_5+\nu_9$  band but this was limited to 17 strong  $^2Q$  lines while thousands of lines are overlapping in this region. Let us mention, the detection of 2500  $C_2H_4$  lines in the high sensitivity CRDS study of acetylene [22]. Indeed, the  $\nu_5+\nu_9$  band of  $C_2H_4$  is located in a region of very weak absorption of  $C_2H_2$  and ethylene with a 5 ppm relative concentration was found to dominate the acetylene spectrum near  $6150\text{ cm}^{-1}$ . In Ref. [22], devoted to the analysis of the acetylene spectrum, an FTS spectrum of  $C_2H_4$  was recorded in order to discriminate the  $C_2H_4$  lines. An empirical line list of more than 18000 ethylene lines with absolute intensity values was systematically retrieved (but not published) in the  $5800 - 6400\text{ cm}^{-1}$  region, thus including the  $\nu_5+\nu_9$  band. This line list is included on the lower panel of **Fig. 1**.

From the above discussion, it appears that our present experimental knowledge of the ethylene spectrum at high resolution is far to be sufficient to fulfill needs for a number of (exo)planetary and astrophysical applications including simulations of absorption and emission spectra, radiative and non-LTE processes, in particular at high temperature. Because they are complete and provide the temperature dependence of the line intensities, calculations appear to be the most suitable approach to fulfill these needs [23-29]. Recently, comprehensive ethylene line lists (TheoReTS lists, hereafter) were calculated up to  $5200\text{ cm}^{-1}$  for the temperatures 50-700 K, based on accurate *ab initio* potential and dipole moment surfaces and extensive first-principle calculations [26]. The 700 K list computed up to  $J = 71$  contains almost 60 million lines with intensities larger than  $5 \times 10^{-27}\text{ cm/molecule}$ . From validation tests against PNNL spectra of ethylene at medium resolution, the calculated list was found in very good agreement with experiments up to  $6400\text{ cm}^{-1}$  (although calculated line positions cannot have experimental accuracy).

In the present analysis, the current TheoReTS line list is extended up to  $9000\text{ cm}^{-1}$  (see **Fig. 1**). One of the goals of the present work is to test the quality of this new variational list near  $7000\text{ cm}^{-1}$  and to evaluate to which extent the calculated list can be used for the assignments of the ethylene spectra newly recorded by FTS up to  $9000\text{ cm}^{-1}$ . These FTS spectra were recorded at four temperatures (130, 201, 240 and 297 K) and two pressures for each temperature value. Indeed, the ethylene saturation pressure remains relatively high at low temperature (about 10 Torr at 120 K) allowing for a valuable reduction of the spectral congestion by cooling. In the  $6700-7260\text{ cm}^{-1}$  region, line parameters will be systematically retrieved from the 130 K spectrum. The availability of spectra at various temperatures will allow for an empirical determination of the lower state energy of the transitions ( $E_{emp}$ ) from the dependence of the line intensities with temperature.

The remaining part of the paper is organized as follows. In the following section, we describe the experimental setup and the conditions of the FTS recordings. The fitting process and construction of the line list are presented in section 3. Section 4 describes the assignment process by comparison to the Variational line list together with a discussion of the obtained results. In particular, the comparison

of the empirically determined  $E_{emp}$  values to their variational counterpart of the assigned lines will provide valuable information (section 5).

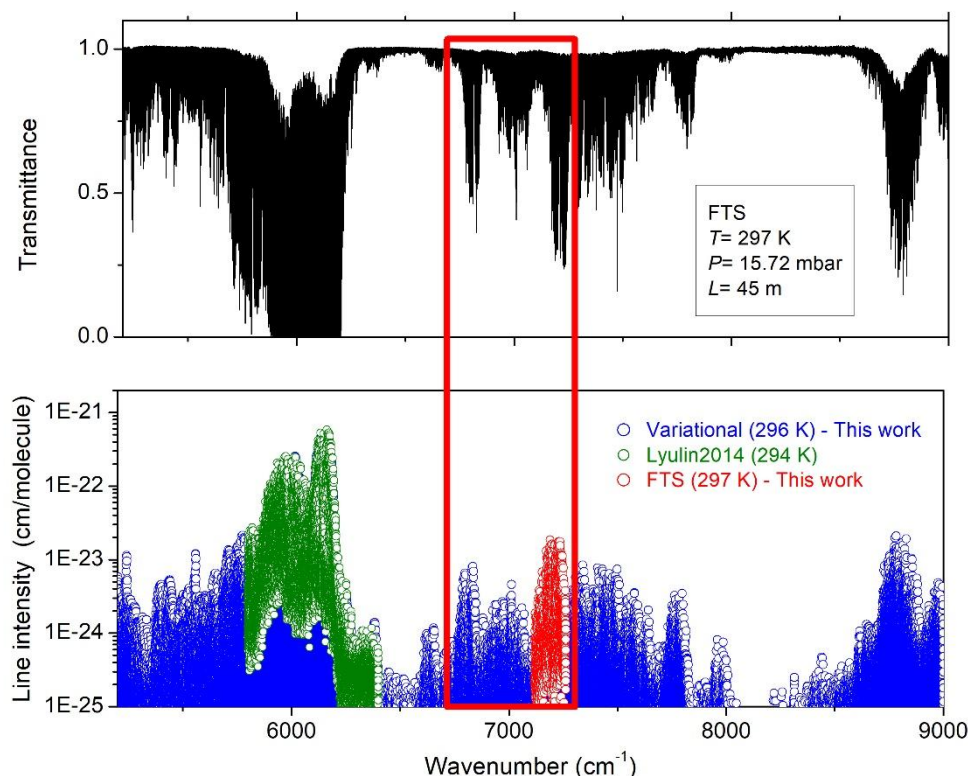


**Figure 1**

Overview of the ethylene spectrum at room temperature in the 5200-9000  $\text{cm}^{-1}$  interval.

*Upper panel:* FTS spectrum recorded at a pressure of 15.72 mbar with a 45 m absorption pathlength (the red rectangle corresponds to the spectral interval analyzed in this work from the spectra recorded at 130 K),

*Lower panel:* variational line list (blue) and experimental list at room temperature elaborated in Ref. [22] and in this work (green and red circles, respectively).

## 2. Experimental details

Eight absorption spectra of ethylene (Air Liquide, stated purity  $\geq 99.95\%$ ) were recorded with a Bruker IFS 125 HR high-resolution Fourier transform spectrometer (FTS) using the cryogenic long path optical cell located on the AILES beamline of the SOLEIL synchrotron [30]. The instrument was fitted with a tungsten source, an entrance aperture set to 1.0 mm, a Si/CaF<sub>2</sub> beam splitter, a high pass filter ( $>3000 \text{ cm}^{-1}$ ), and an InSb detector cooled down to 77 K. The pressures were measured with Pfeiffer capacitance manometers of 10 and 100 mbar full-scale range, temperature stabilized at 45°C and characterized by an accuracy of reading of 0.1%. In our experimental setup, the pressure gauge is located outside the cell, about 80 cm away from the cold valve sealing the gas during the measurement. As a result, at low temperature and for low pressures (less than a few mbar) the measured pressure value does not coincide with the pressure in the cell, due to thermomolecular

effects [31-34]. The following spectra analysis will allow to evidence this bias and to determine a reasonable value of the real pressure in the cell.

An optical path length of 45 m, corresponding to 30 passes was adopted. The spectra were successively recorded at 130(3) K, 201(2) K, 240(1) K and 297(1) K. About four to five days were needed to achieve a 130 K temperature with a 3 K temperature gradient. For each temperature, spectra were recorded for two pressure values as given in **Table 1**. All the interferograms were recorded with a maximum optical path difference (MOPD) of 120 cm, corresponding to a spectral resolution of  $0.0075\text{ cm}^{-1}$  ( $0.9/\text{MOPD}$ , according to the Bruker definition of the spectral resolution) and were transformed without apodization function (Boxcar option) with a zero-filling factor of 8. The number of interferograms averaged to yield the single beam spectra is provided in **Table 1**. The transmittance spectra were obtained after division by a zero-absorption spectrum recorded with the cell evacuated and a  $0.075\text{ cm}^{-1}$  spectral resolution. The recordings cover the range  $3500\text{ to }9000\text{ cm}^{-1}$  but are mostly dedicated to the  $5000\text{-}9000\text{ cm}^{-1}$  range where the absorption amplitude allows for quantitative measurements (below  $5000\text{ cm}^{-1}$ , the absorption is very strong). An overview of the spectrum recorded at 4.15 mbar is displayed on **Fig. 2**, which includes successive zooms illustrating the high spectral congestion remaining at low temperature.

Accurate calibration of the frequency axis was achieved by using two high resolution  $\text{N}_2\text{O}$  spectra (see **Table 1**) and 35 accurate reference line positions provided in the HITRAN database (uncertainties in the  $10^{-3}\text{-}10^{-4}\text{ cm}^{-1}$  range). After calibration, an RMS deviation of the position differences of about  $3\times 10^{-4}\text{ cm}^{-1}$  was achieved.

**Table 1.**

Experimental conditions of the FTS recordings of ethylene between  $5000\text{ and }9000\text{ cm}^{-1}$ . The two last spectra of  $\text{N}_2\text{O}$  were performed for calibration purposes of the ethylene spectra. The spectra #1,2 and 7 are those considered in the present analysis.

#	Temperature (K)	Pressure <sup>a</sup> (mbar)	Path length (m)	Number of scans
<b>1</b>	<b>130(3)</b>	<b>4.15</b>	<b>45</b>	<b>1628</b>
<b>2</b>	<b>130(3)</b>	<b>0.25</b>	<b>45</b>	<b>2416</b>
3	201(2)	5.82	45	1258
4	201(2)	0.31	45	592
5	240(1)	8.19	45	296
6	240(1)	0.48	45	1554
<b>7</b>	<b>297(1)</b>	<b>15.72</b>	<b>45</b>	<b>1232</b>
8	297(1)	0.64	45	888
9	297(1)	3.34 ( $\text{N}_2\text{O}$ )	69	1628
10	130(3)	$\sim 0.042$ ( $\text{N}_2\text{O}$ )	45	888

<sup>a</sup> At low temperature, the pressure given by the gauge is an underestimated value of the real pressure in the cell (see Text).

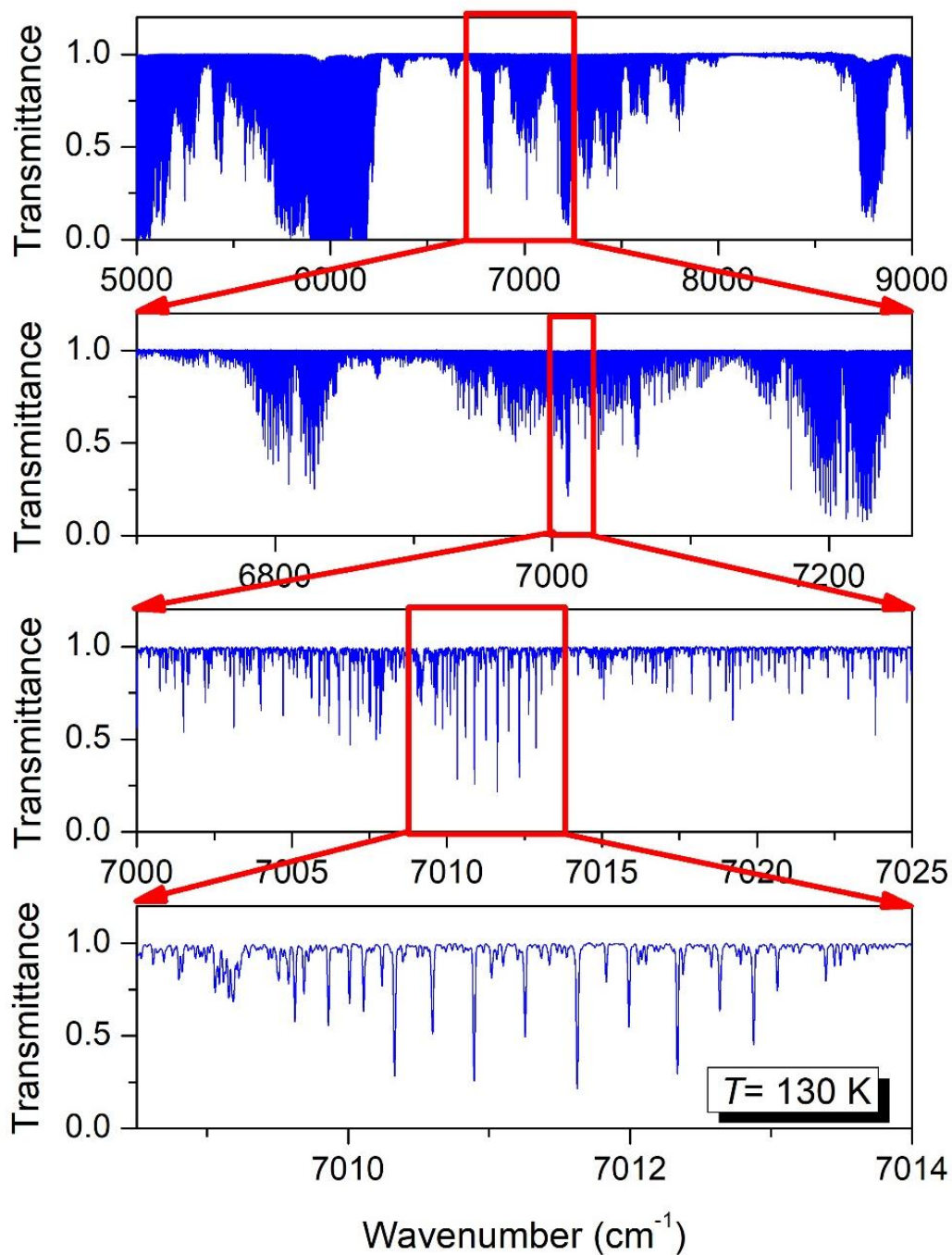


**Figure 2**

Overview of the Fourier transform absorption spectrum of ethylene at 130 K in natural isotopic abundance recorded with a spectral resolution of  $0.0075 \text{ cm}^{-1}$ . The upper panel illustrates the whole spectrum. The second panel corresponds to the region analyzed in the present work. The absorption pathlength was 45 m and the pressure was about 4.15 mbar.



### 3. Line list construction

In the present work, we limited our analysis to the 6700-7260  $\text{cm}^{-1}$  interval (red rectangle in **Fig. 2**). Due to the high spectral congestion, the 130 K spectra (#1 and #2 in **Table 1**) were first considered. A line list at room temperature was also elaborated in the 7120-7260  $\text{cm}^{-1}$  interval from the spectrum #7 (see lower panel in **Fig. 2**) in order to evaluate to which extent the lower state energy level can be empirically determined from the variation of the line intensity between 130 K and 297 K ( $2T$ -method, [35-39]).

#### 3.1. The 7120-7260 $\text{cm}^{-1}$ interval at 130 K and 297 K

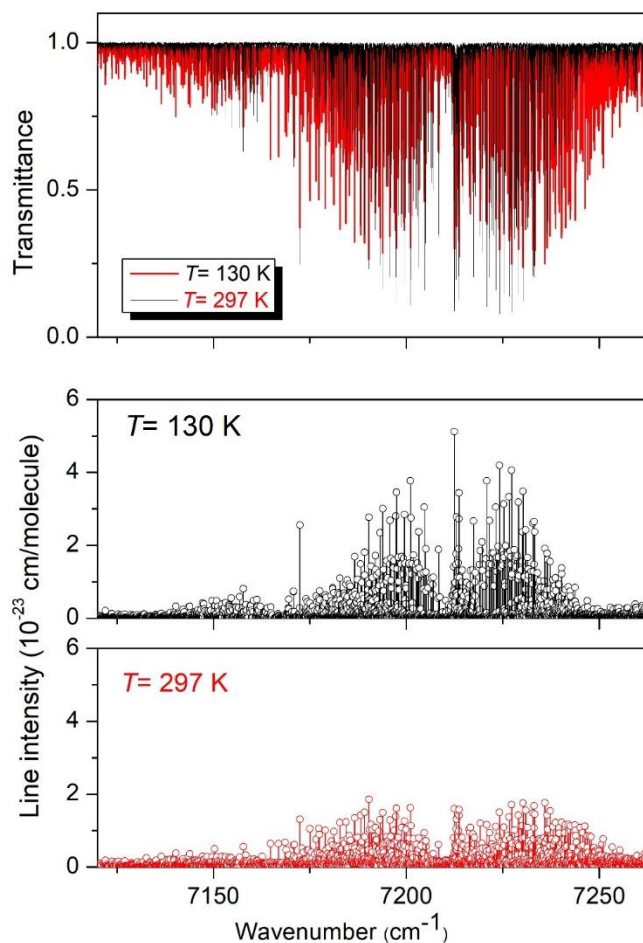


**Figure 3.**

Fourier transform absorption spectrum of ethylene at 130 K and 297 K recorded with a spectral resolution of  $0.0075 \text{ cm}^{-1}$  (black and red, respectively). The absorption pathlength was 45 m. The pressure was 15.72 mbar at 297 K and about 4.15 mbar at 130 K. The corresponding lists are displayed on the two lower panels.

Let us first consider the 130 K spectra (#1 and #2 in **Table 1**) and the spectrum #7 at 297 K in the 7120-7260  $\text{cm}^{-1}$  interval. The overview of the 130 K (#1) and 297 K (#7) spectra is presented in **Fig. 3**. The strongest lines at 130 K being close to saturation in spectrum #1, their line parameters were replaced by those retrieved from the spectrum #2 at 0.25 mbar. The line centers and intensities were determined using an interactive least squares multi-line fitting program

(<http://sourceforge.net/projects/fityk/> version v 1.1.1). The fit was performed assuming a simple Voigt function as line profile, thus, including in an effective way the Instrument Line Shape (ILS). In practice, the spectrum was divided into successive spectral segments for which a linear function was adjusted to account for the baseline. **Figure 4** shows an example of the simulation of the experimental spectra at 130 K and 297 K in a same spectral interval near  $7219 \text{ cm}^{-1}$ . Note the temperature dependence of the line intensities and the reduction of the spectral congestion at 130 K. The line intensity,  $S_{\nu_0}$  (cm/molecule), of a rovibrational transition centred at  $\nu_0$  was obtained from the integrated line absorbance,  $A_{\nu_0}$  ( $\text{cm}^{-1}$ ):

$$A_{\nu_0}(T) = \int_{line} \alpha_{\nu} L d\nu = \int_{line} \ln \left[ \frac{I_0(\nu)}{I(\nu)} \right] d\nu = S_{\nu_0}(T) NL \quad (1)$$

where:  $\frac{I_0(\nu)}{I(\nu)}$  is the ratio of the incident intensity to the transmitted intensity,

$L$  is the absorption pathlength in cm,

$\nu$  is the wavenumber in  $\text{cm}^{-1}$ ,

$\alpha(\nu)$  is the absorption coefficient in  $\text{cm}^{-1}$ ,

$N$  is the molecular concentration in molecule/ $\text{cm}^3$  obtained from the measured pressure value:  $P = NkT$ .

A typical value of about  $5 \times 10^{-3}$  is achieved for the RMS deviation of the experimental and simulated absorbances. This *rms* value corresponds to a Noise Equivalent Absorption of about  $\alpha_{min} \approx 1 \times 10^{-6} \text{ cm}^{-1}$  and minimum line strength values on the order of  $10^{-25} \text{ cm/molecule}$  for the spectrum recorded at 4.15 mbar and 130 K.

The 130 K global line list was obtained by combining the line lists derived at 4.15 and 0.25 mbar (spectrum #1 and #2, respectively). In general, lines with intensities larger than  $4 \times 10^{-24} \text{ cm/molecule}$  were taken from the list at 0.25 mbar while the list at 4.15 mbar was used for the weaker lines. Around this intensity threshold an average value of the line parameters was adopted. In **Fig. 3**, the resulting list at 130 K (3114 lines) is presented together with the 297 K list (2276 lines derived from spectrum #7). As expected, a reduction of the range of the rotational structure of the dominant band centered near  $7210 \text{ cm}^{-1}$  is observed at low temperature. In addition, the strongest lines corresponding to low values of the lower state energy level have a significantly higher absolute intensity at 130 K. In  $\text{C}_2\text{H}_4$ , cooling down to 130 K leads to an intensity increase by a factor 3.5 of the transitions from the ground state ( $E_{emp} = 0$ ) and a decrease by about a factor of 6 for those with lower state energy of about  $500 \text{ cm}^{-1}$ .

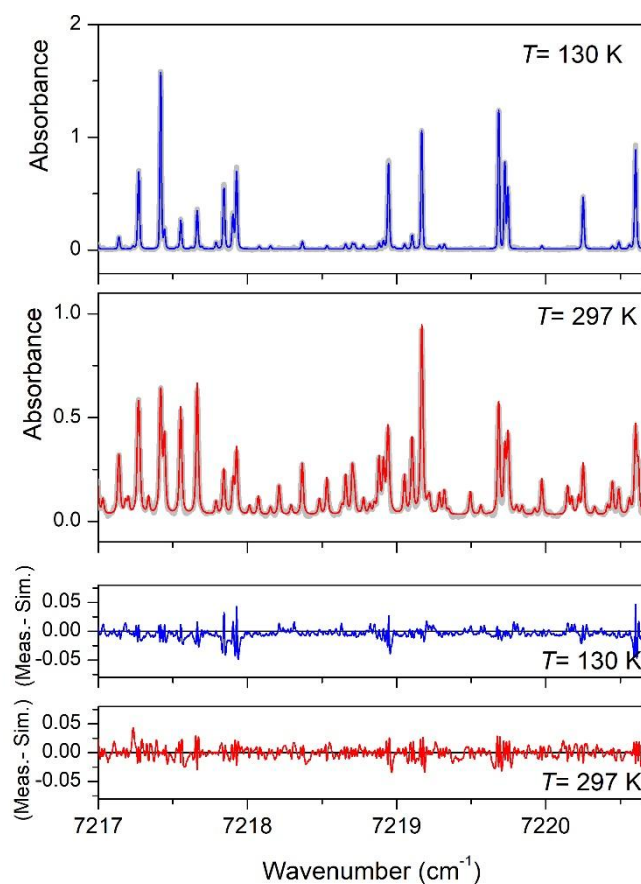


**Figure 4.**

Line parameter retrieval from the FTS spectra of ethylene at 130 K ( $P= 4.15$  mbar) and 297 K ( $P= 15.72$  mbar) near  $7219\text{ cm}^{-1}$  (blue and red, respectively). For each temperature, the best fit spectrum is superimposed to the measured spectrum and the corresponding residuals are displayed on the lower panels.

**Table 2.** Amount of  $\text{C}_2\text{H}_4$  lines retrieved in this work with corresponding intensities at 130 K and 297 K and comparison to the variational list [26].

	FTS		variational [26] <sup>b</sup>	
	Nb	Sum of intensities (cm/molecule)	Nb	Sum of intensities (cm/molecule)
<b>7120 - 7260 <math>\text{cm}^{-1}</math></b>				
130K	3114/1465 <sup>a</sup>	$5.46 \times 10^{-21} / 4.67 \times 10^{-21}$ <sup>a</sup>	6585	$4.51 \times 10^{-21}$
297 K	2276/1465 <sup>a</sup>	$4.28 \times 10^{-21} / 3.55 \times 10^{-21}$ <sup>a</sup>	6564	$3.31 \times 10^{-21}$
<b>6700 - 7260 <math>\text{cm}^{-1}</math></b>				
130 K	12310	$1.22 \times 10^{-20}$	19141	$1.00 \times 10^{-20}$

*Notes*

<sup>a</sup> The second value corresponds to the subset of 1465 transitions with lower state energy determined by the  $2T$ -method,

<sup>b</sup> The intensity cut-off of the variational list is  $10^{-25}$  cm/molecule.

The intensity of an absorption line is proportional to the population of the lower state energy and the temperature dependence of the intensities is thus that of the Boltzmann factor. Consequently,

the value of the lower state energy of a given transition,  $E_{emp}$ , can be determined experimentally from the ratio of its line intensity at two temperatures [15,16]:

$$\frac{S_{\nu_0}(T_1)}{S_{\nu_0}(T_0)} = \frac{Z(T_0)}{Z(T_1)} \exp \left[ -E_{emp} \left( \frac{1}{kT_1} - \frac{1}{kT_0} \right) \right] \quad (2)$$

where  $S_{\nu_0}$  and  $Z$  are the line intensities and partition functions, respectively, and  $T_0 = 297$  K and  $T_1 = 130$  K in our case. Following previous studies by Margolis [35], we have extensively used this  $2T$ -method to derive  $E_{emp}$  values of methane transitions in the near infrared [36-39]. The corresponding values of the partition function were taken from the HITRAN database for  $^{12}\text{C}_2\text{H}_4$  [13]:

$$\frac{Z(297 \text{ K})}{Z(130 \text{ K})} = 3.641 \cdot$$

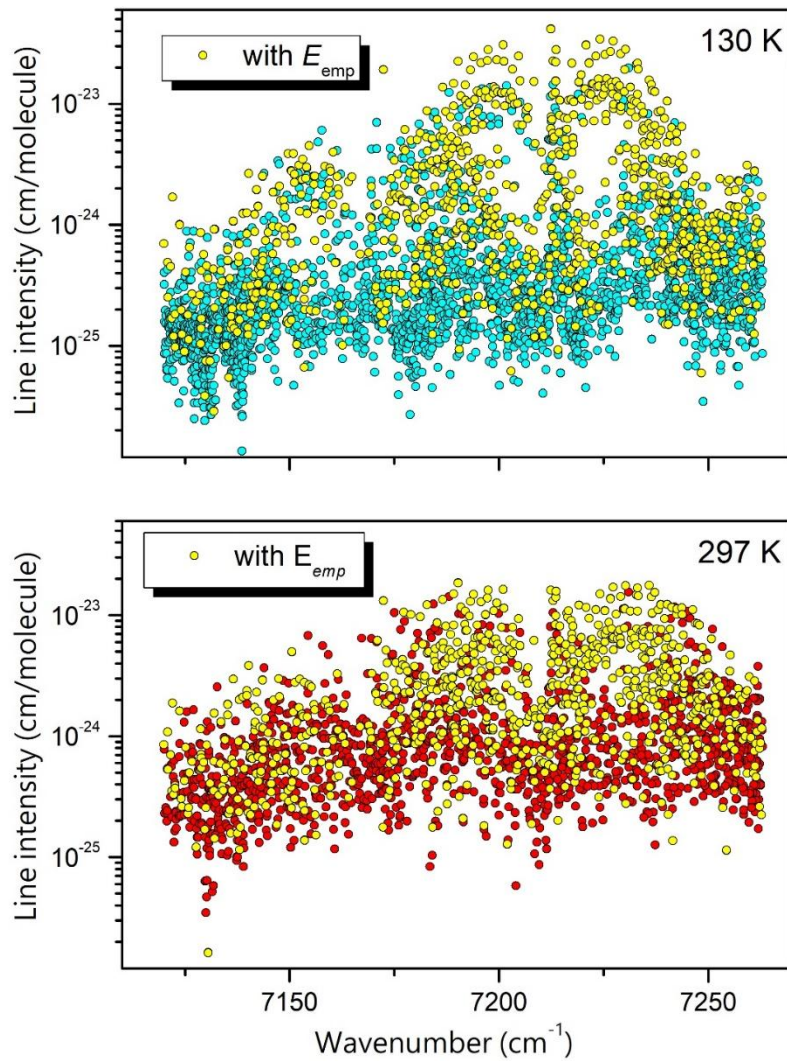


**Fig. 5**

Overview of the line lists at 130 K and 297 K in the 7120 - 7260  $\text{cm}^{-1}$  interval.

Empirical values of the lower state energy were derived by the  $2T$ -method for the lines of the 297 K and 130 K lists with positions coinciding within  $0.003 \text{ cm}^{-1}$ . These lines are highlighted by yellow dots.

Lines corresponding to the same transition in the 297 K and 130 K lists were associated using the position agreement as only criterion. In order to avoid accidental coincidences, we fixed to  $0.003 \text{ cm}^{-1}$  the maximum value of the difference,  $\delta$ , of the 297 K and 130 K line centers. This value was chosen according to the estimated uncertainties on the two line centers and corresponds to about one fifth of the Doppler width (about  $0.0168 \text{ cm}^{-1}$  FWHM in our region) at 297 K. Overall, 1469 pairs of lines were found to fulfil the  $\delta < 0.003 \text{ cm}^{-1}$  criterion allowing for the derivation of the corresponding lower state energies (Eq. 2). The associated transitions are highlighted in **Fig. 5** and represent 85.5 and 82.9 % of the total absorption measured at 130 K and 297 K, respectively (see **Table 2**). The complete list of the 2276 transitions measured at 297 K is provided as Supplementary Material. For the 1465 transitions with  $E_{\text{emp}}$  values, we include the  $E_{\text{emp}}$  values together with the experimental values of the position and the intensity of the 130 K counterpart. A similar Supplementary Material is provided for the 3115 lines measured at 130 K.

In the case of methane, due to the large value of the rotational constant ( $B_0 = 5.214 \text{ cm}^{-1}$ ), the overwhelming majority of the transitions observed at room temperature are cold band transitions with a lower state rotational quantum  $J$ , less than 12. In other words, methane line intensities have no more than twelve ways to vary with temperature. Consequently, a quality test of the  $E_{\text{emp}}$  values provided by the  $2T$ -method is to check if their obtained values are close to the twelve possible  $B_0 J(J+1)$  values or equivalently if the corresponding  $J_{\text{emp}}$  values are close to integers. The clear propensity of the  $J_{\text{emp}}$  values to be integer was systematically checked in our  $\text{CH}_4$  studies using the  $2T$ -method [38-41]. In the case of the  $\text{C}_2\text{H}_4$  asymmetric top molecule, the ground state rotational energies can have much more distinct values and their energy separation is much smaller which makes the comparison with the derived  $E_{\text{emp}}$  values not informative.

In the following, we will show that part of the measured  $\text{C}_2\text{H}_4$  transitions can be reliably assigned by comparison to the variational line list. When possible, the lower state energy value of the assigned transitions were compared to the obtained  $E_{\text{emp}}$  values providing a stringent test on the quality of the  $E_{\text{emp}}$  values. Unfortunately, large and numerous discrepancies were noted between our  $E_{\text{emp}}$  values and their  $E_{\text{var}}$  counterpart. In order to clarify the situation, we extrapolated the intensities measured at 297 K to 130 K using the  $E_{\text{var}}$  values of the assigned transitions. As a result, the extrapolated intensity values were found systematically higher by about 23 % than measured. This systematic bias points a difference between the pressure value given by our pressure gauge and the pressure on the cooled cell, the latter being value being about 23% higher. After correction of the 130 K line intensities according to this correct cell pressure (3.37 mbar instead of 4.15 mbar), the corrected  $E_{\text{emp}}$  values were found in reasonable agreement with the  $E_{\text{var}}$  values. As an illustration of the temperature dependence of the spectrum, **Fig. 6** presents a comparison between the 130 K and 297 K spectra. The derived  $E_{\text{emp}}$  values are indicated.

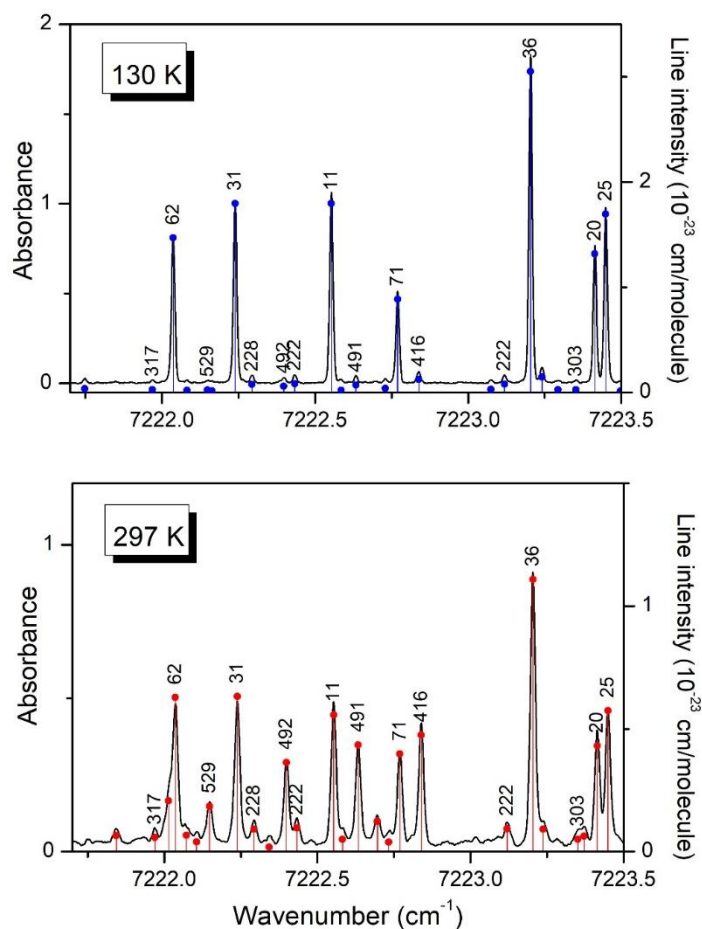


**Fig. 6**

Derivation of the lower state empirical energy values,  $E_{emp}$ , by application of the  $2T$ -method to the FTS spectra of ethylene at 130 and 297 K (upper and lower panel, respectively). The derived  $E_{emp}$  values (in  $\text{cm}^{-1}$ ) are indicated for lines with centers coinciding within  $2 \times 10^{-3} \text{ cm}^{-1}$ . The blue and red dots correspond to the line intensities (right-hand scale).

### 3.2. The 6700-7260 $\text{cm}^{-1}$ line list at 130 K

In view of testing the variational line list over a larger spectral interval, the 130 K list was extended down to  $6700 \text{ cm}^{-1}$  using the spectrum at 4.15 mbar. The extended 130 K list is provided as a separate Supplementary Material. **Fig. 7** presents an overview comparison of the experimental list to the corresponding variational list at 130 K.

## 4. Rovibrational assignments based on the variational list

### 4.1. The variational line list between 5200 and 9000 $\text{cm}^{-1}$

In Ref. [26], complete and comprehensive ethylene line lists were obtained from accurate *ab initio* potential and dipole moment surfaces (PES [23] and DMS [24], respectively) and extensive first-principle calculations. Three lists spanning the  $0$ - $6400 \text{ cm}^{-1}$  infrared region were built at  $T = 80, 160,$  and  $296 \text{ K}$ , and two lists in the range  $0$ - $5200 \text{ cm}^{-1}$  were built at  $500$  and  $700 \text{ K}$ . These lists are freely accessible at <http://theorets.univ-reims.fr> and <http://theorets.tsu.ru> web sites. In this work, the calculations were extended up to  $9000 \text{ cm}^{-1}$ , using the same PES and DMS. The resulting lists at 130

K and 296 K are provided as Supplementary Material attached to the present paper. For each temperature, the intensity cutoff was fixed to  $1 \times 10^{-25}$  cm/molecule.

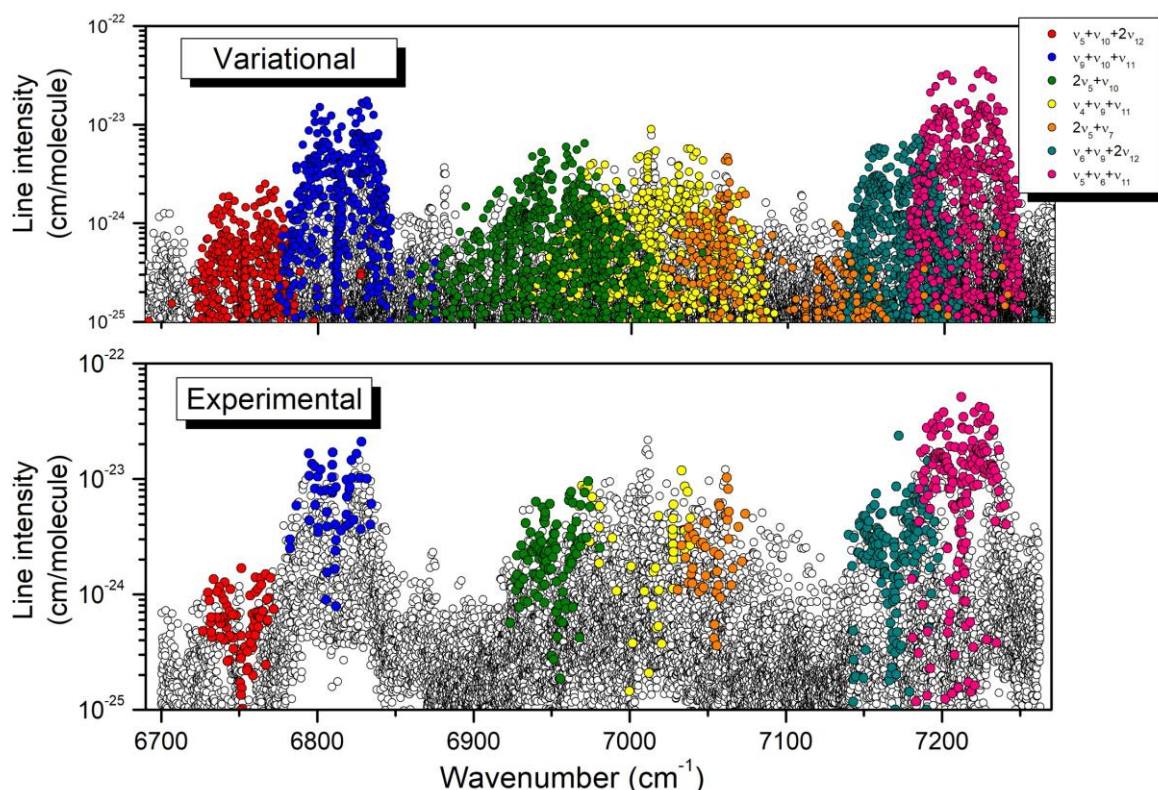


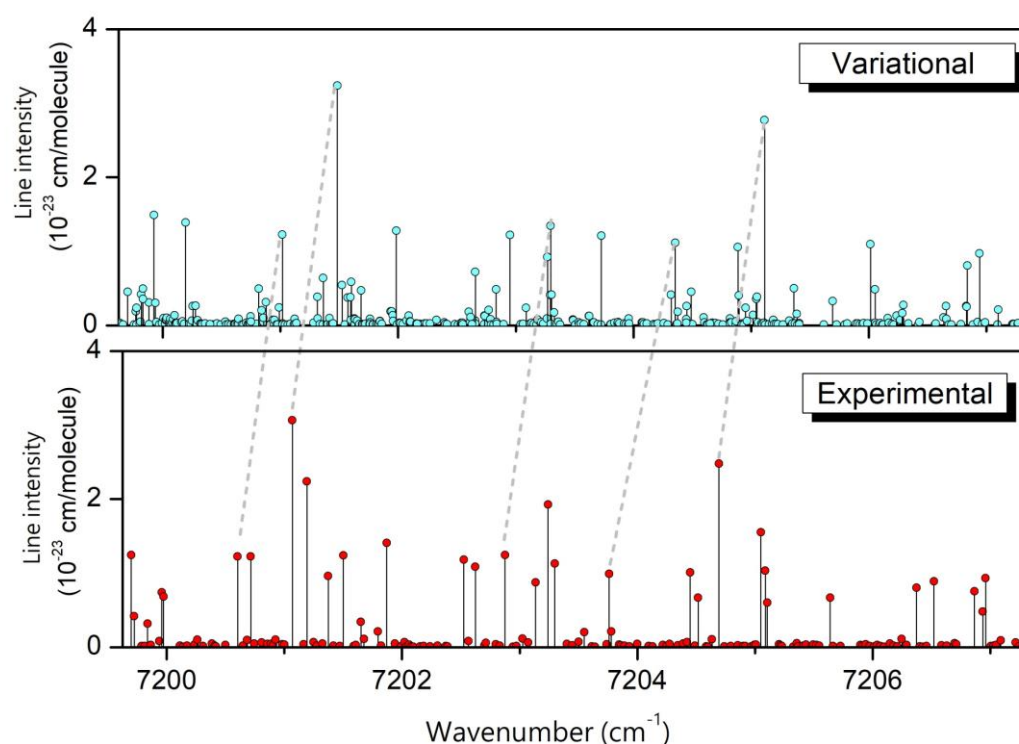
**Fig. 7**

Overview of the experimental and variational line lists at 130 K in the 6700 - 7260  $\text{cm}^{-1}$  interval. Seven bands included in the variational list are highlighted on the upper panel. Some of the transitions of each band could be assigned in the experimental list and are highlighted on the lower panel.

#### 4.2. Rovibrational assignments by comparison to the variational line list between 6700 and 7260 $\text{cm}^{-1}$

The overview of our 130 K line list shows a good agreement with the corresponding variational list (**Fig. 7**). Nevertheless, this overall agreement which is obvious at the scale of the overview is much less clear at a larger scale and a one-to-one correspondence between the experimental and calculated transitions is far to be straightforward (see a typical situation in **Fig. 8**). The accuracy of the variational positions and intensities combined with a high spectral congestion made impossible to have the rovibrational assignments exclusively based on the position and intensity agreement of the experimental and variational values. In that situation, Lower State Combination Difference (LSCD) relations were used as the key criterion. (Let us recall that the LSCD is the difference of the frequencies of two transitions reaching the same upper energy level). In each region, the dominant band was first identified in the variational list. Seven bands highlighted on the upper panel of **Fig. 7** were considered in the region. In each band, the transitions sharing the same upper state (*e.g.* involved in LSCD relations) were grouped. Then, the comparison to the strongest experimental lines in the

region allowed to identify the most probable candidate corresponding to a given variational transition. The variational assignment of the candidate line was validated only if it was confirmed by the observation of at least a second experimental line involved in a LSCD relation. The LSCD criterion was considered as fulfilled when the experimental and TheoReTs LSCD values coincided within  $4 \times 10^{-3} \text{ cm}^{-1}$ . A similar way to fulfil the LSCD relation is to check that the frequency shift of the variational position from its experimental value is identical (within  $4 \times 10^{-3} \text{ cm}^{-1}$ ) for the candidate line and its LSCD counterpart.



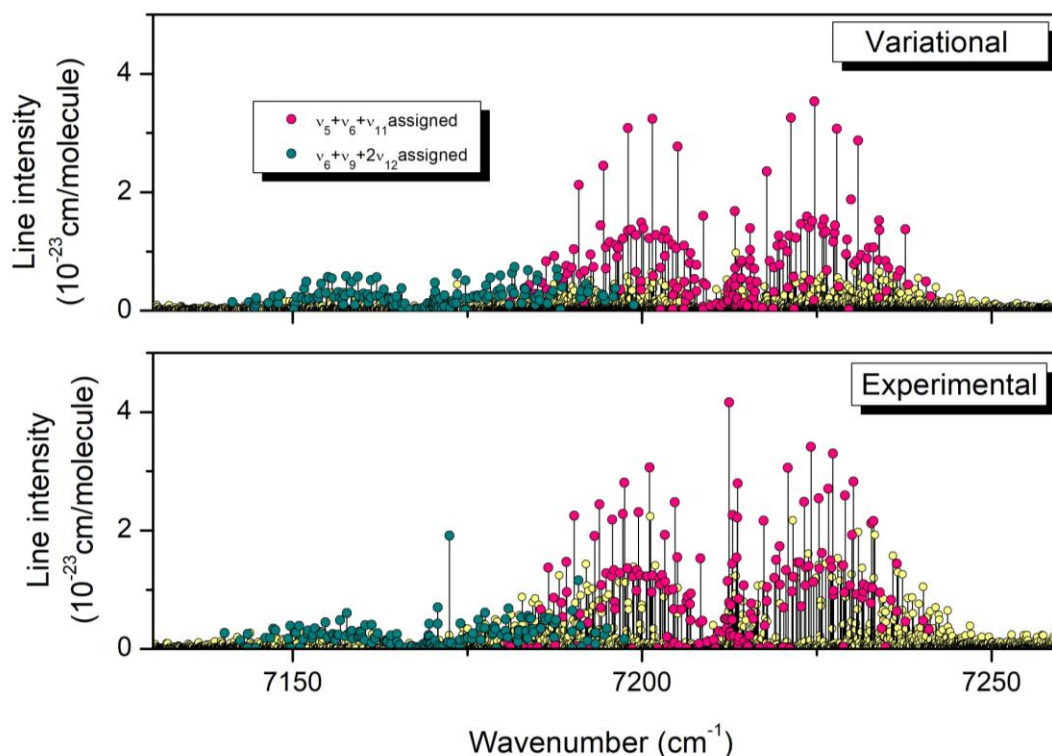
**Fig. 8**

Illustration of the difficulties of the assignments of the ethylene spectrum at 130 K near  $7202 \text{ cm}^{-1}$ . The FTS spectrum and corresponding line list (lower panel) are compared to the variational line list used for the assignments (upper panel). The dashed lines link corresponding lines of the variational and FTS datasets.

We present in **Fig. 9**, the variational and experimental line lists at 130 K in the region of the  $\nu_6+\nu_9+2\nu_{12}$  and  $\nu_5+\nu_6+\nu_{11}$  bands ( $7140\text{-}7250 \text{ cm}^{-1}$ ). For most of the strong and medium lines of the region, a variational counterpart was identified allowing for a transfer of the rovibrational assignment to the experimental line. Overall, 647 transitions of seven bands were assigned between  $6700$  and  $7260 \text{ cm}^{-1}$ . They are highlighted on the lower panel of **Fig. 7**, while on the upper panel all the variational transitions of the seven considered bands are highlighted. The experimental positions and intensities of the assigned lines can be found in the variational list at 130K provided as Supplementary Material. The statistics of the assignments are summarized in **Table 3**. According to the band, the sum of the variational intensities of the assigned lines represents between 17 and 79 % of the total



variational band intensities. Overall the total intensity of the assigned transitions represents 25 % and 29 % of the total TheoReTs and experimental intensities in the region, respectively. Indeed, as illustrated in **Fig. 7**, a large fraction of the transitions including strong lines remains unassigned. In particular, only a few transitions could be assigned to the  $\nu_4+\nu_9+\nu_{11}$  band near  $6995\text{ cm}^{-1}$  while at the scale of **Fig. 7**, the general appearance of the rotational structure of this band looks similar to the observations. This is partly a consequence of our choice to have all the assignments supported by LSCD relations.



**Fig. 9**

Rovibrational assignments in the  $\nu_6+\nu_9+2\nu_{12}$  and  $\nu_5+\nu_6+\nu_{11}$  bands of  $\text{C}_2\text{H}_4$ .

*Upper panel:* Variational line list at 130 K. The assigned transitions of the  $\nu_5+\nu_6+\nu_{11}$  and  $\nu_6+\nu_9+2\nu_{12}$  bands are indicated (pink and dark cyan dots, respectively). Lines belonging to unassigned transitions of the same bands and to other bands are also included (yellow dots)

*Lower panel:* Experimental list with assigned transitions of the  $\nu_5+\nu_6+\nu_{11}$  and  $\nu_6+\nu_9+2\nu_{12}$  bands highlighted (pink, dark cyan and yellow symbols correspond to  $\nu_5+\nu_6+\nu_{11}$  and  $\nu_6+\nu_9+2\nu_{12}$  and unassigned transitions, respectively).

**Table 3**

Statistics of the  $^{12}\text{C}_2\text{H}_4$  transitions assigned to seven bands in the absorption spectrum at 130 K in the  $6700 - 7260\text{ cm}^{-1}$  interval and comparison to the variational list.

Band	Variational			Assigned lines			
	Band center ( $\text{cm}^{-1}$ )	Nb	Int. sum ( $\text{cm}/\text{molecule}$ )	Nb	Int. sum ( $\text{cm}/\text{molecule}$ )		
					Exp.	Var.	Exp./Var.
$\nu_5+\nu_{10}+2\nu_{12}$	$6752.21(J_{up}=0)$	362	$1.62\times 10^{-22}$	78	$5.12\times 10^{-23}$	$7.16\times 10^{-23}$	0.72
$\nu_9+\nu_{10}+\nu_{11}$	$6814.08(J_{up}=0)$	413	$1.03\times 10^{-21}$	50	$3.71\times 10^{-22}$	$3.19\times 10^{-22}$	1.16
$2\nu_5+\nu_{10}$	$6948.14(J_{up}=0)$	720	$5.44\times 10^{-22}$	103	$2.58\times 10^{-22}$	$2.1\times 10^{-22}$	1.23

$v_4+v_9+v_{11}$	$6994.73(J_{up}=2)$	694	$5.46 \times 10^{-22}$	45	$1.68 \times 10^{-22}$	$9.35 \times 10^{-23}$	1.80
$2v_5+v_7$	$7053.38(J_{up}=0)$	224	$1.13 \times 10^{-22}$	42	$1.18 \times 10^{-22}$	$4.42 \times 10^{-23}$	2.67
$v_6+v_9+2v_{12}$	$7167.41(J_{up}=0)$	674	$6.95 \times 10^{-22}$	156	$4.95 \times 10^{-22}$	$3.8 \times 10^{-22}$	1.30
$v_5+v_6+v_{11}$	$7210.61(J_{up}=0)$	449	$1.8 \times 10^{-21}$	173	$2.12 \times 10^{-21}$	$1.42 \times 10^{-21}$	1.49
<b>Total</b>		<b>3536</b>	<b><math>4.89 \times 10^{-21}</math></b>	<b>647</b>	<b><math>3.58 \times 10^{-21}</math></b>	<b><math>2.54 \times 10^{-21}</math></b>	<b>1.40</b>

In Fig. 10, the deviations between the variational and experimental line positions are plotted *versus* the energy of the upper state. As all upper states are involved in LSCD relations, various energy determinations are available (up to six for some upper levels of transitions of the  $v_4+v_9+v_{11}$  band). On this figure, we limited to three the number of superimposed symbols corresponding to distinct determinations. Overall, the deviations range between  $-3.8 \text{ cm}^{-1}$  and  $+3.5 \text{ cm}^{-1}$ . Although each band exhibits some outliers, the general tendency is a decrease of the  $(v_{\text{meas.}} - v_{\text{var.}})$  values with the upper state energy indicating that, apart a global vibrational shift corresponding to the first rotational levels, the rotational energy of the upper state appears to be systematically overestimated by the variational calculations, the overestimation increasing with the rotational energy. This effect is probably related to the convergence of the variational calculations which is less and less complete as  $J$  increases.

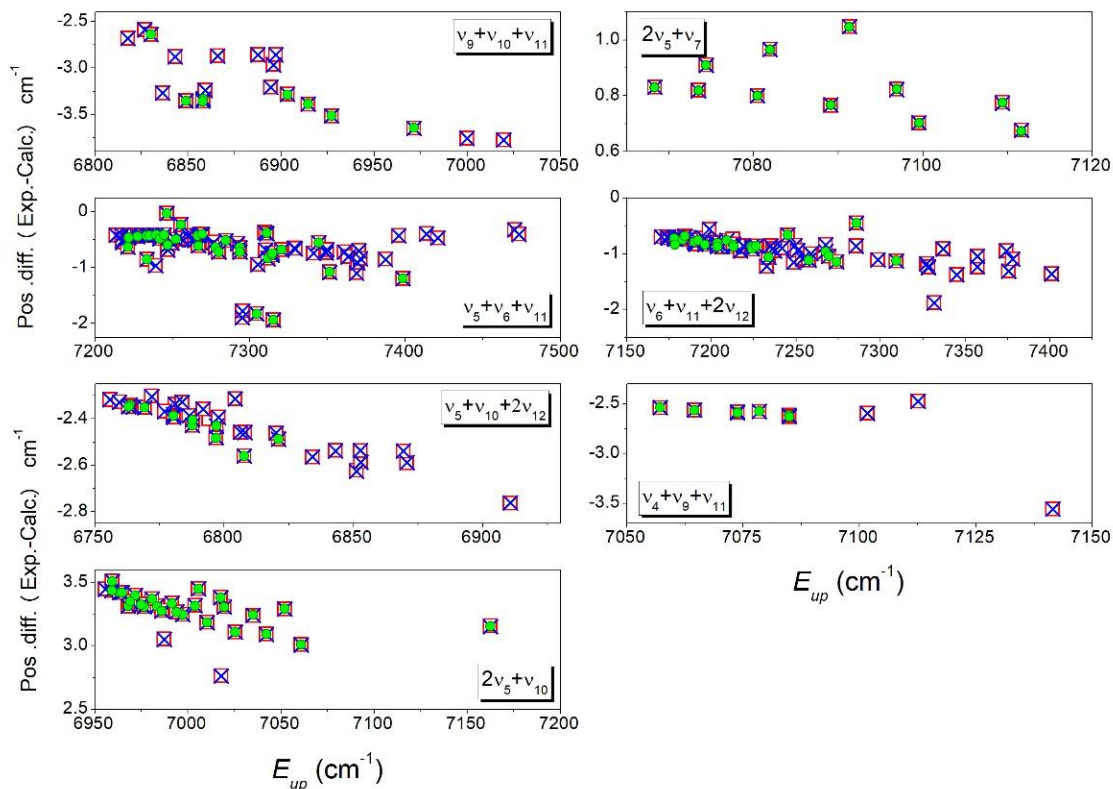


**Fig. 10**

Differences between the measured and variational line positions *versus* the energy of the upper state for the  $^{12}\text{C}_2\text{H}_4$  transitions assigned in the FTS spectrum at 130 K in the 6700-7260  $\text{cm}^{-1}$  interval.

Different symbols are superimposed corresponding to various determinations of the same upper level energy through different transitions.

The band-by-band comparison of the measured intensities to variational values show an overall reasonable agreement. The  $S_{meas.}/S_{var}$  intensity ratios show a large dispersion around an average value not far from unity for all the bands. According to the values included in **Table 3**, the intensity of the assigned lines are on average 40% larger than calculated, the  $\nu_4+\nu_9+\nu_{11}$  the  $2\nu_5+\nu_{10}$  band intensity being overestimated by about 2 and 3, respectively.

## 5. Conclusion

This contribution is a first step towards an improvement of our knowledge of the complex ethylene spectrum in the near infrared (5000-9000  $\text{cm}^{-1}$ ). On the basis of a series of high resolution spectra recorded at four temperatures between 130 K and 297 K, empirical line lists were constructed. A list of more than 19000 absorption lines at 130 K is provided for the 6700 - 7260  $\text{cm}^{-1}$  region. To the best of our knowledge this is the first extensive experimental list of ethylene lines including intensities constructed above 5000  $\text{cm}^{-1}$  (The intensities of only 17 strong  $^oQ$  lines of the  $\nu_5+\nu_9$  band near 6150  $\text{cm}^{-1}$  were reported in Ref. [19] while the list of 18000 lines constructed in the 5800 - 6400  $\text{cm}^{-1}$  region in Ref. [22] was not published). The application of the  $2T$ -method to experimental lists at 130 K and 297 K have allowed to derive the empirical value of the lower state energy of 1465 transitions in the 7120 - 7260  $\text{cm}^{-1}$  interval. This method is valuable to account for the temperature dependence of the ethylene absorption spectrum but is of limited help to assign and model the  $\text{C}_2\text{H}_4$  spectrum in the region. As a test of the extrapolation capabilities of the calculations of the  $^{12}\text{C}_2\text{H}_4$  spectrum from *ab initio* PES and DMS, the TheoReTS calculations of Ref. [26] were extended up to 9000  $\text{cm}^{-1}$  and calculated line lists at 296 K and 130 K are provided as Supplementary Materials. Although important deviations (up to a few  $\text{cm}^{-1}$  for line positions) were noted, the calculated line list was found sufficiently accurate to allow for reliable rovibrational assignments of about 650 lines belonging to seven bands of the considered 6700 - 7260  $\text{cm}^{-1}$  region. These assignments were systematically validated by LSCD relations between several (up to six) transitions sharing the same upper state. Undoubtedly, a more in-depth analysis of such dense and rich experimental spectra could benefit in a near future from the construction of an effective model based on the PES and DMS, as proposed in Ref. [26]. It would allow refining quite easily some diagonal Hamiltonian parameters such as band centers or rotational constants and accounting for all dark states which are usually omitted in the ordinary empirical effective approach.

The procedure used to assign the high resolution  $\text{C}_2\text{H}_4$  spectrum by comparison to the variational is very similar to that encountered for another medium-size molecule,  $\text{NH}_3$ , for which a high number of transitions could be recently assigned in the 3900-6350  $\text{cm}^{-1}$  region [42-44] on the basis of the ExoMol variational line lists [45,46] (see also similar procedure followed in Refs. [47,48] for  $\text{NH}_3$  assignments based on the Ames theoretical line list). The computing tools developed for the

assignment of the  $\text{NH}_3$  spectra could advantageously be used to transfer the variational assignments to the large of FTS data at disposal. Note that in the present work, our analysis of the ethylene spectra relied exclusively on the variational list newly extended up to  $9000\text{ cm}^{-1}$  and we did not consider the ExoMol line list which is available up to  $7000\text{ cm}^{-1}$  [28,29]. As an illustration of the limitations of the theoretical line lists and of the present difficulty to use them to assign the ethylene spectrum in the near infrared, we compare the variational, ExoMol and experimental lists at  $130\text{ K}$  in **Fig. 11**, in two spectral intervals. Around  $6808\text{ cm}^{-1}$  (left panels), the experimental spectrum (at  $130\text{ K}$ ) exhibits regular series of lines which correspond most probably to  $^{\text{Q}}\text{Q}$ -branches of the  $\nu_9+\nu_{10}+\nu_{11}$  band centered near  $6814.08\text{ cm}^{-1}$ . The variational and ExoMol lists predict quite different spectra in the region but both do not show any spectral regularity or obvious correlation with the experimental spectrum. In the region of the  $\nu_5+\nu_{10}+2\nu_{12}$  band centered at  $6752.21\text{ cm}^{-1}$  (right panels), the ExoMol calculated spectrum shows a quite regular rotational structure in disagreement with the observations. This may indicate that a number of resonance interactions were missed in the ExoMol calculations. The variational spectrum is more irregular but a one-to-one correspondence with the experimental spectrum is very difficult and only 78 transitions could be assigned to this band. These two examples illustrate the present gap between the best today theoretical predictions and the observations. Further improvements of the theoretical calculations appear to be the most efficient way to assign extensively the ethylene spectrum in the near infrared.

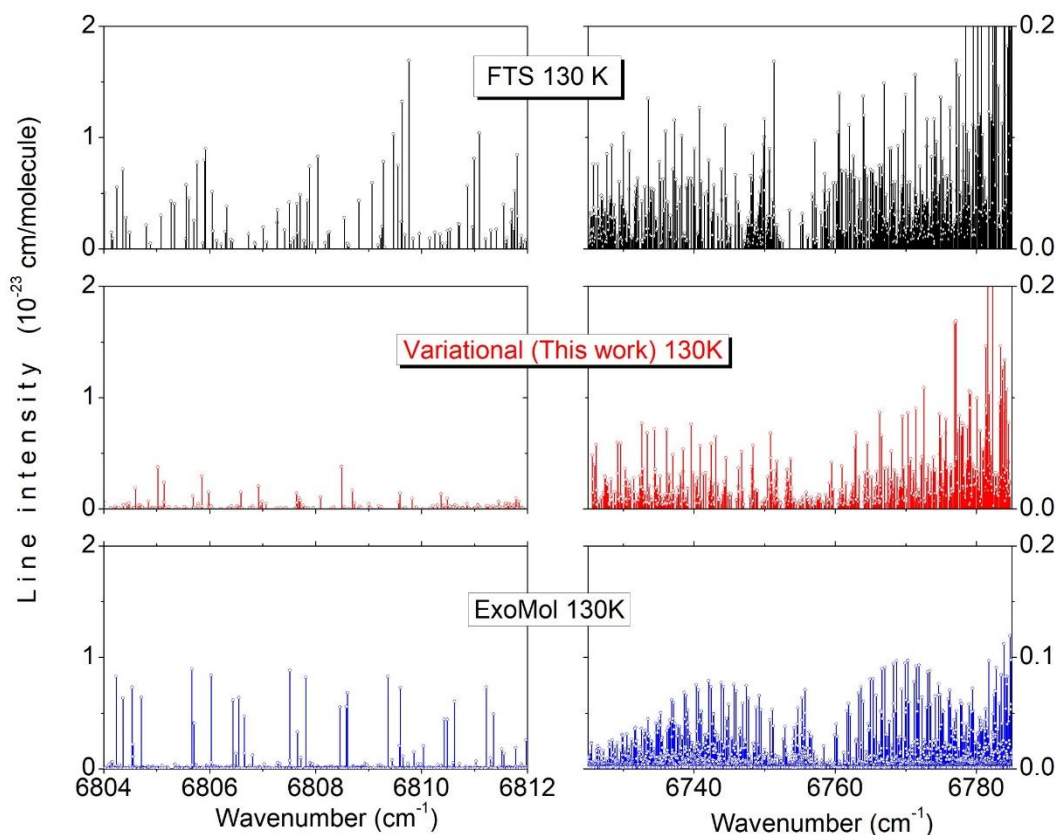


**Fig. 11**

Comparison of the experimental list of ethylene at 130 K obtained in this work to the TheoReTs and ExoMol calculated lists [28,29].

Left panels:  $^{\circ}\text{Q}$ -branches of the  $\nu_9+\nu_{10}+\nu_{11}$  band centered near  $6814.08\text{ cm}^{-1}$

Right panels:  $\nu_5+\nu_{10}+2\nu_{12}$  band centered at  $6752.21\text{ cm}^{-1}$

*Acknowledgements*

*We acknowledge funding from the Agence Nationale de la Recherche (e\_PYTHeAS ANR-16-CE31-0005 and ANR-RNF TEMMEX-ANR-21-30 CE-0053-01). MR acknowledges support from the Romeo computer center of Reims Champagne-Ardenne.*

## References

1. Goode JG, Yokelson RJ, Susott RA, Ward DE. Trace gas emissions from laboratory biomass fires measured by open-path Fourier transform infrared spectroscopy: Fires in grass and surface fuels. *J Geophys Res Atmos* 1999;104:21237.
2. Rinsland CP, Paton-Walsh C, Jones NB, et al. High spectral resolution solar absorption measurements of ethylene (C<sub>2</sub>H<sub>4</sub>) in a forest fire smoke plume using HITRAN parameters: Tropospheric vertical profile retrieval. *J Quant Spectr Rad Transf* 2009;96:301-9.
3. Kostiuik T, Romani P, Espenak F, Livengood T, Goldstein J. Temperature and abundances in the jovian auroral stratosphere:2. Ethylene as a probe of the microbar region. *J Geophys Res* 1993;98:18823-30. <https://doi.org/10.1029/93JE01332>
4. Romani PN, Jennings DE, Bjoraker GL, Sada PV, McCabe GH, Boyle RJ. Temporally varying ethylene emission on Jupiter. *Icarus* 2008;198:420-34. <https://doi.org/10.1016/j.icarus.2008.05.027>
5. Bézard B, Moses J, Lacy J, Greathouse T, Richter M, Griffith C. Detection of ethylene (C<sub>2</sub>H<sub>4</sub>) on Jupiter and Saturn in non-auroral regions. *Bull Am Astron Soc* 2000;33:1079.
6. Hesman BE, Bjoraker GL, Sada PV, et al. Elusive ethylene detected in Saturn's northern storm region. *The Astrophysical Journal* 2012;760. <https://doi.org/10.1088/0004-637X/760/760/1/24>
7. Rey M. Novel methodology for systematically constructing global effective models from ab initio-based surfaces:a new insight into high-resolution molecular spectra analysis. *J Chem Phys* 2022;156:224103. <https://doi.org/10.1063/5.0089097>
8. Vervack Jr RJ, Sandel B, Strobel D. New perspectives on Titan's upper atmosphere from a re-analysis of the Voyager 1 UVS solar occultations. *Icarus* 2004;170:91–112. <https://doi.org/10.1016/j.icarus.2004.03.005>
9. Roe H, de Pater I, McKay CP. Seasonal variation of Titan's stratospheric ethylene (C<sub>2</sub>H<sub>4</sub>) observed. *Icarus* 2004;169:440-461. <https://doi.org/10.1016/j.icarus.2004.01.002>
10. Coustenis A, Achterberg RK, Conrath BJ, Jennings DE, Marten A, Gautier D, et al. The composition of Titan's stratosphere from Cassini/CIRS mid-infrared spectra. *Icarus* 2007;189:35-62. <https://doi.org/10.1016/j.icarus.2006.12.022>
11. Vinatier S, Bézard B, Fouchet T, et al. Vertical abundance profiles of hydrocarbons in Titan's atmosphere at 15° S and 80° N retrieved from Cassini/CIRS spectra. *Icarus* 2007;188:120. <https://doi.org/10.1016/j.icarus.2006.10.031>
12. Canosa A, Paramo A, Le Picard SD, Sims IR. An experimental study of the reaction kinetics of C<sub>2</sub>(X<sup>1</sup>Σ<sup>g+</sup>) with hydrocarbons (CH<sub>4</sub>, C<sub>2</sub>H<sub>2</sub>, C<sub>2</sub>H<sub>4</sub>, C<sub>2</sub>H<sub>6</sub> and C<sub>3</sub>H<sub>8</sub>) over the temperature range 24–300 K: Implications for the atmospheres of Titan and the Giant Planets. *Icarus* 2007;187:558. <https://doi.org/10.1016/j.icarus.2006.10.009>
13. Gordon IE, Rothman LS, Hargreaves RJ, Hashemi R, Karlovets EV, Skinner FM, et al. The HITRAN2020 molecular spectroscopic database. *J Quant Spectrosc Radiat Transf* 2022;277:107949. <https://doi.org/10.1016/j.jqsrt.2021.107949>
14. Duncan J L, Ferguson AM. Local mode and normal mode interpretations of the CH and CD stretching vibrational manifolds in C<sub>2</sub>H<sub>4</sub> and C<sub>2</sub>D<sub>4</sub>. *J Chem Phys* 1988;89 (7):4216–4226. <https://doi.org/10.1063/1.454806>
15. Rossi A, Buffa R, Scotony M, Bassi D, Iannotta S, Boschetti A. Optical enhancement of diode laser-photoacoustic trace gas detection by means of external Fabry–Perot cavity. *Appl Phys Lett* 2005;87:041110. <https://doi.org/10.1063/1.2000341>
16. Boschetti A, Bassi D, Iacob E, Iannotta S, Ricci L, Scotoni M. Resonant photoacoustic simultaneous detection of methane and ethylene by means of a 1.63-μm diode laser. *Applied Physics B* 2002;74:273-278. <https://doi.org/10.1007/s003400200790>

17. Bach M, Georges R, Herman M, Perrin A. Investigation of the fine structure in overtone absorption bands of  $^{12}\text{C}_2\text{H}_4$ . *Mol Phys* 1999;97:265–77. <https://doi.org/10.1080/00268979909482828>
18. Platz T, Demtroder W. Sub-doppler optothermal overtone spectroscopy of ethylene and dichloroethylene. *Chem Phys Lett* 1998;294(4–5):397–405. [https://doi.org/10.1016/S0009-2614\(98\)00885-9](https://doi.org/10.1016/S0009-2614(98)00885-9)
19. Parkes AM, Lindley RE, Orr-Ewing AJ. Absorption cross-sections and pressure broadening of rotational lines in the  $\nu_5+\nu_9$  band of ethane measured by diode laser cavity ring down spectroscopy. *Phys Chem Chem Phys* 2004;6:5313–7. <https://doi.org/10.1039/B413238F>
20. Kapitanov VA, Ponomarev YuN. High resolution ethylene absorption spectrum between 6035 and 6210  $\text{cm}^{-1}$ . *Appl Phys B* 2008;90:235–41. <https://doi.org/10.1007/s00340-007-2920-3>
21. Loroño Gonzalez MA, Boudon V, Loëte M, Rotger M, Bourgeois M-T, Didriche K, Herman M, Kapitanov VA, Ponomarev YuN, Solodov AA, Solodov AM, Petrova TM. High-resolution spectroscopy and preliminary global analysis of C–H stretching vibrations of  $\text{C}_2\text{H}_4$  in the 3000 and 6000  $\text{cm}^{-1}$  regions. *J Quant Spectrosc Radiat Transf* 2010;111:2265–2278. <https://doi.org/10.1016/j.jqsrt.2010.04.010>
22. Lyulin OM, Mondelain D, Béguier S, Kassi S, Vander Auwera J, Campargue A. High sensitivity absorption spectroscopy of acetylene by CRDS between 5851 and 6341  $\text{cm}^{-1}$ . *Mol Phys* 2014;112:2433–44. <https://doi.org/10.1080/00268976.2014.906677>
23. Delahaye T, Nikitin AV, Rey M, Szalay PG, Tyuterev VIG. A new accurate ground-state potential energy surface of ethylene and predictions for rotational and vibrational energy levels. *J Chem Phys* 2014;141:104301. <https://doi.org/10.1063/1.4894419>
24. Delahaye T, Nikitin AV, Rey M, Szalay PG, Tyuterev VIG. Accurate 12D dipole moment surfaces of ethylene. *J Chem Phys* 2015;639:275–282. <https://doi.org/10.1016/j.cplett.2015.09.042>
25. Rey M, Chizhmakova IS, Nikitin AV, Tyuterev VIG. Understanding global infrared opacity and hot bands of greenhouse molecules with low vibrational modes from first-principles calculations: the case of  $\text{CF}_4$ . *J Chem Phys* 2018;20:21008–21033. <https://doi.org/10.1039/C8CP03252A>
26. Rey M, Delahaye T, Nikitin AV, Tyuterev VG. First theoretical global line lists of ethylene ( $^{12}\text{C}_2\text{H}_4$ ) spectra for the temperature range 50–700 K in the far-infrared for quantification of absorption and emission in planetary atmospheres. *Astron Astrophys* 2016;594:A47. doi:10.1051/0004-6361/201629004.
27. D. Viglaska, M. Rey, T. Delahaye, A.V. Nikitin. First-principles calculations of infrared spectra for three ethylene isotopologues:  $^{13}\text{C}_2\text{H}_4$ ,  $^{13}\text{C}^{12}\text{CH}_4$  and  $^{12}\text{C}_2\text{H}_3\text{D}$ , *J Quant Spectrosc Radiat Transfer* 2019;230:142–54.
28. Mant BP, Yachmenev A, Tennyson J, Yurchenko SN, ExoMol molecular line lists - XXVII: spectra of  $\text{C}_2\text{H}_4$ , *Monthly Notices of the Royal Astronomical Society* 2018;478:3220–32.
29. Tennyson J et al. The ExoMol database: Molecular line lists for exoplanet and other hot atmospheres, *J Mol Spectrosc*, 2016;327,73–94. <https://doi.org/10.1016/j.jms.2016.05.002>.
30. KwabiaTchana F, Willaert F, Landsheere X, Flaud J-M, Lago L, Chapuis M, Roy P, Manceron L. A new, low temperature long-pass cell for mid-infrared to terahertz spectroscopy and synchrotron radiation use. *Rev Sci Instrum* 2013;84:093101. <https://doi.org/10.1063/1.4819066>.
31. Takaishi T, Sensui Y. Thermal transpiration effect of hydrogen, rare gases and methane. *Farad Trans. Royal Soc* 1963;59:2503.
32. Roberts TR, Sydoriak SG. Thermomolecular Pressure Ratios for He3 and He4. *Phys Rev* 1956;102:304
33. Tanuma H, Fujimatsu H, Kobayashi N. Ion mobility measurements and thermal transpiration effects in helium gas at 4.3 K. *J Chem Phys* 2000;113:1738.

34. Gobeille RF, Mantz AW. Corrections to measured sample pressures in low temperature collisional cooling experiments. *Spectrochim Acta A* 2002;58:2421.
35. Margolis JS. Empirical values of the ground state energies for methane transitions between 5500 and 6150  $\text{cm}^{-1}$ . *J Appl Opt* 1990;29:2295-302. doi:10.1364/AO.29.002295.
36. Kassi S, Gao B, Romanini D, Campargue A. The near-infrared (1.30–1.70  $\mu\text{m}$ ) absorption spectrum of methane down to 77 K. *Phys Chem Chem Phys* 2008;10:4410–4419. doi:10.1039/B805947K.
37. Campargue A, Wang L, Kassi S, Mašát M, Votava O. Temperature dependence of the absorption spectrum of  $\text{CH}_4$  by high resolution spectroscopy at 81 K:(II) The Icosad region (1.49-1.30  $\mu\text{m}$ ). *J Quant Spectrosc Radiat Transfer* 2010;111(9):1141-51. <https://doi.org/10.1016/j.jqsrt.2009.11.025>
38. Sciamma-O'Brien E, Kassi S, Gao B, Campargue A. Experimental low energy values of  $\text{CH}_4$  transitions near 1.33 $\mu\text{m}$  by absorption spectroscopy at 81K. *J Quant Spectrosc Radiat Transf* 2009;110(12);951-963. <https://doi.org/10.1016/j.jqsrt.2009.02.004>
39. Wang L, Mondelain D, Kassi S, Campargue A. The absorption spectrum of methane at 80 and 294 K in the icosad (6717-7589  $\text{cm}^{-1}$ ): Improved empirical line lists, isotopologue identification and temperature dependence. *J Quant Spectrosc Radiat Transfer* 2012;113(1):47–57. <https://doi.org/10.1016/j.jqsrt.2011.09.003>
40. Campargue A, Leshchishina O, Wang L, Mondelain D, Kassi S. The WKLMC empirical line lists (5852-7919  $\text{cm}^{-1}$ ) for methane between 80 K and 296 K: final lists for atmospheric and planetary applications. *J Molec Spectrosc* 2013;291:16–22.
41. Campargue A, Leshchishina O, Mondelain D, Kassi S, Coustenis A. An improved empirical line list for methane in the region of the 2  $\nu_3$  band at 1.66  $\mu\text{m}$ . *J Quant Spectrosc Radiat Transfer* 2013;118:49–59.
42. Cacciani P, Čermák P, Béguier S, Campargue A. The absorption spectrum of ammonia between 5650 and 6350  $\text{cm}^{-1}$ . *J. Quant Spectrosc Radiat Transf* 2021;258:107334. <https://doi.org/10.1016/j.jqsrt.2020.107334>
43. Cacciani P, Čermák P, Vander Auwera J, Campargue A. The ammonia absorption spectrum between 3900 and 4700  $\text{cm}^{-1}$ . *J. Quant Spectrosc Radiat Transf* 2022;277:107961. doi:10.1016/j.jqsrt.2021.107961
44. Cacciani P, Čermák P, Vander Auwera J, Campargue A. The ammonia absorption spectrum between 4700 and 5650  $\text{cm}^{-1}$ . *J. Quant Spectrosc Radiat Transf* 2022;292:108250. doi:/10.1016/j.jqsrt.2022.108350
45. Coles PA, Ovsyannikov RI, Polyansky OL, Yurchenko SN, Tennyson J. Improved potential energy surface and spectral assignments for ammonia in the near-infrared region. *J Quant Spectrosc Radiat Transf* 2018;219:199–212. doi:10.1016/j.jqsrt.2018.07.022.
46. Coles PA., Yurchenko SN, Tennyson J, ExoMol molecular line lists – XXXV. A rotation-vibration line list for hot ammonia. *Monthly Notices of the Royal Astronomical Society* 2019;490:4638-47. doi.org/10.1093/mnras/stz2778
47. Huang X, Sung K, Toon JC, Schwenke DW., Lee TJ A collaborative  $^{14}\text{NH}_3$  IR spectroscopic analysis at 6000  $\text{cm}^{-1}$ . *J. Quant Spectrosc Radiat Transf* 2022;280:108076. doi:/10.1016/j.jqsrt.2022.108076
48. Sung K, Brown LR, Huang X, Schwenke DW, Lee TJ, Coy SL, et al. Extended line positions, intensities, empirical lower state energies and quantum assignments of  $\text{NH}_3$  from 6300 to 7000  $\text{cm}^{-1}$ . *J Quant Spectrosc Radiat Transf* 2012;113:1066–83. doi:10.1016/j.jqsrt.2012.02.037.